Molecular insights into the corrosion inhibition performance of Sclerocarya birrea leaf phytochemicals on aluminum: a combined DFT and Monte Carlo simulation study

Phenyo Shathani*

Department of Chemical, Materials and Metallurgical Engineering, Faculty of Engineering, Botswana International University of Science and Technology, Palapye, Botswana

*Corresponding Author:
Email*:
sp22017778@studentmail.biust.ac.bw

Revised: February 12, 2026
Accepted: Mei 29, 2026

DOI: 10.1980/jses.v1i1.5

Phone*: +26776525305

Abstract: *This study presents a computational investigation of bioactive compounds derived from Sclerocarya birrea leaf extract as potential green corrosion inhibitors for aluminum. Four major constituents, namely Ethanol,2-(octadecyloxy) (T1), Hexadecanoic acid ethyl ester (T2), Octadecanoic acid ethyl ester (T3), and Octadecanoid acid (T4), were evaluated using Density Functional Theory (DFT) and Monte Carlo simulations. Electronic descriptors, including EHOMO, ELUMO, energy gap (ΔE), electronegativity, hardness, and electron transfer fraction (ΔN), were analyzed to determine inhibition performance. Monte Carlo simulations further revealed strong adsorption interactions between the inhibitor molecules and the aluminum surface. Among the investigated compounds, T1 exhibited the highest adsorption energy and the most favorable electronic properties, indicating superior corrosion inhibition performance. The predicted inhibition efficiency follows the order T1 > T3 > T2 > T4, consistent with both quantum chemical and adsorption results. The findings demonstrate that Sclerocarya birrea-derived compounds are promising sustainable corrosion inhibitors and confirm the effectiveness of integrated computational approaches for predicting corrosion inhibition behavior.*

Keywords: *Aluminium, corrosion inhibitor, Sclerocarya birrea, DFT, Monte Carlo simulation*

Introduction

Aluminum and its alloys are indispensable engineering materials widely employed in aerospace, marine, transportation, and structural industries due to their high strength-to-weight ratio, thermal and electrical conductivity, recyclability, and fabrication versatility [1], [2]. Their intrinsic corrosion resistance arises from the spontaneous formation of a compact oxide film (Al_2O_3) that acts as a protective barrier against environmental attack [3]. However, this passive layer exhibits amphoteric characteristics and becomes unstable in aggressive acidic or alkaline environments, leading to film dissolution and accelerated electrochemical degradation [3], [4]. Consequently, despite its favorable properties, aluminum remains susceptible to corrosion under harsh service conditions [4].

Corrosion is fundamentally an electrochemical process involving anodic metal dissolution coupled with cathodic reduction reactions in the presence of an electrolyte [5]. Beyond material degradation, corrosion generates severe economic, safety, and environmental consequences, including infrastructure failure, process inefficiency, contamination risks, and high maintenance costs. Global economic analyses consistently demonstrate that corrosion-related losses account for a significant percentage of industrial GDP, underscoring the urgent need for effective mitigation strategies [6]. Among available approaches, corrosion inhibitors remain one of the most practical and cost-effective solutions due to their operational simplicity and adaptability to existing industrial systems [5], [7].

Traditional inorganic and synthetic organic inhibitors often provide high inhibition efficiency but are increasingly restricted due to toxicity, environmental persistence, and regulatory concerns [8]. This limitation has stimulated extensive research into sustainable and biodegradable alternatives. Plant-derived extracts have emerged as promising green corrosion inhibitors because they contain diverse secondary metabolites rich in heteroatoms (N, O, S), aromatic rings, and conjugated systems capable of interacting with metal surfaces through donor–acceptor mechanisms [9]–[11]. Adsorption of such organic molecules onto metallic substrates typically reduces active surface area and suppresses anodic and/or cathodic reactions [10], [11].

Among medicinal plants with rich phytochemical composition, Sclerocarya birrea (Marula) has attracted attention due to the presence of long-chain fatty acid derivatives, esters, alcohols, phenolics, and other bioactive constituents [12], [13]. Functional groups such as hydroxyl, carbonyl, and ether linkages in these compounds provide potential adsorption centers that may enhance corrosion inhibition performance, since adsorption is strongly influenced by heteroatoms and π-electron systems [14], [15]. Although several experimental studies have investigated plant extracts as corrosion inhibitors, systematic computational evaluation of individual phytochemical derivatives from Sclerocarya birrea, particularly toward aluminum surfaces, remains limited. Moreover, mechanistic insight into structure–reactivity–adsorption relationships is still insufficiently explored [14], [16].

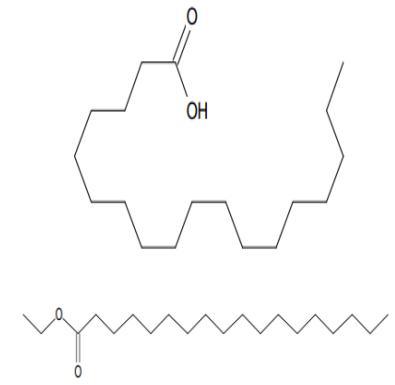

a) Octadecanoic acid
b) octadecanoic acid, ethyl ester

c) Ethanol, 2-(octadecyloxy)
d) Hexadecanoic acid, ethyl ester

Figure 1 (a – d). Chemical structures of the four derivatives of *Sclerocarya birrea* ethanolic leaf extract.

In recent years, computational chemistry has become a powerful predictive tool in corrosion science. Density Functional Theory (DFT) enables quantitative assessment of electronic parameters governing inhibitor reactivity, such as frontier molecular orbital energies (EHOMO and ELUMO), energy gap (ΔE), ionization potential, electron affinity, electronegativity (χ), global hardness (η), and electron transfer fraction (ΔN) [14], [15]. These descriptors provide insight into electron-donating and electron-accepting abilities, which directly influence adsorption strength [17]. When combined with statistical simulation techniques such as Monte Carlo (MC) modeling, it becomes possible to investigate adsorption configurations, binding energies, and thermodynamic stability at the metal–inhibitor interface [18], [19]. The integration of quantum chemical calculations and surface simulations allows rational screening of corrosion inhibitors prior to experimental validation, thereby reducing time, cost, and material usage [16].

Despite growing interest in green inhibitors, few studies have applied a multiscale simulation framework to evaluate specific phytochemical derivatives from Sclerocarya birrea extract for aluminum corrosion inhibition. A predictive, mechanism-oriented investigation that correlates molecular electronic structure with adsorption energetics is therefore required. Addressing this gap is particularly important for advancing simulation-driven inhibitor design and enhancing the scientific robustness of plant-based corrosion research [14], [16].

Methodology

Quantum Chemical Calculations

Quantum chemical calculations were performed to elucidate the electronic properties, molecular reactivity, and electron transfer capability of four major derivatives isolated from the ethanolic leaf extract of Sclerocarya birrea: Ethanol,2-(octadecyloxy) (T1), Hexadecanoic acid ethyl ester (T2), Octadecanoic acid ethyl ester (T3), and Octadecanoic acid (T4). The optimized molecular structures are presented in Figure 1.

All molecular geometries were fully optimized using Density Functional Theory (DFT) within the framework of the B3LYP hybrid exchange–correlation functional combined with the 6-31G(d) basis set [20–22]. This level of theory was selected due to its proven reliability in predicting molecular electronic structure and corrosion-related reactivity descriptors while maintaining reasonable computational cost [28], [29]. Frequency calculations were subsequently performed to confirm that the optimized geometries correspond to true minima on the potential energy surface, characterized by the absence of imaginary frequencies.

Geometry optimizations were conducted in the gas phase to ensure computational efficiency and consistency with previous corrosion modeling studies, as solvent effects at

this level of screening are generally reported to exert minimal influence on qualitative electronic trends [28], [29]. All quantum chemical computations were carried out using the Gaussian 09 software package [23].

From the optimized structures, key global reactivity descriptors were determined to assess inhibition potential. Frontier molecular orbital energies, namely the highest occupied molecular orbital (EHOMO) and lowest unoccupied molecular orbital (ELUMO), were calculated to evaluate electron-donating and electron-accepting tendencies [25], [28]. The energy gap (ΔE = ELUMO − EHOMO) was used as an indicator of molecular stability and chemical reactivity [28], [29]. Additional descriptors including ionization potential (I), electron affinity (A), electronegativity (χ), global hardness (η), and the fraction of electron transfer (ΔN) were derived based on Koopmans' approximation and conceptual DFT principles [24], [25].

According to Koopmans' theorem, ionization potential and electron affinity can be approximated from the negative values of EHOMO and ELUMO, respectively [24]:

$$I = -EHOMO \quad (1)$$
$$A = -ELUMO \quad (2)$$

Electronegativity (χ) and hardness (η) of each organic inhibitor can be calculated by Equations (3) and (4) based on conceptual DFT formalism [25]:

$$\chi = ((I+A))/2 \quad (3)$$
$$\eta = ((I-A))/2 \quad (4)$$

According to Pearson's hard and soft acids and bases (HSAB) theory [26], [27], the number of electrons transferred (ΔN) from each organic inhibitor to aluminum metal can be calculated using Equation (5):

$$\Delta N = (\chi Al - \chi Inh)/(2(\eta Al + \eta Inh)) \quad (5)$$

where χAl and χInh represent the absolute electronegativity values of aluminum and the organic inhibitor molecules, respectively. Similarly, ηAl and ηInh denote the absolute hardness values of aluminum and the inhibitor species. The theoretical values χAl=3.23 eV and ηAl=2.77eV were adopted for aluminum to estimate the fraction of electrons transferred (ΔN) between the inhibitor molecules and the metal surface, following the electronegativity equalization principle and conceptual DFT framework [25–27].

Monte Carlo Simulations

Monte Carlo (MC) simulations were performed to investigate the adsorption behavior of the inhibitor molecules on the aluminum surface using Materials Studio 7.0. Prior to surface interaction analysis, all inhibitor structures were geometry-optimized employing the COMPASS (Condensed-phase Optimized Molecular Potentials for Atomistic Simulation Studies) force field to ensure accurate conformational stability and reliable intermolecular interaction parameters.

The adsorption system was constructed using an Al(111) surface slab model, selected due to its thermodynamic stability and relevance in corrosion studies. A periodic supercell of 20 × 20 was generated to minimize boundary effects and ensure sufficient surface area for molecular interaction. A vacuum layer of 15 Å was introduced perpendicular to the surface plane to prevent artificial interactions between periodic images along the z-direction.

The simulation cell consisted of one inhibitor molecule and 100 water molecules to approximate an aqueous environment and account for competitive adsorption effects. Periodic boundary conditions were applied in the x and y directions. The adsorption process was explored through stochastic sampling to identify energetically favorable configurations, and the most stable adsorption geometry was determined based on minimum adsorption energy criteria.

Adsorption energy (E_ads) was calculated to quantify the interaction strength between inhibitor molecules and the Al(111) surface. A more negative adsorption energy indicates stronger surface affinity and enhanced inhibition potential. The MC simulation results provide insight into adsorption orientation, surface coverage behavior, and interfacial stability, complementing the quantum chemical reactivity analysis.

Result and Discussion

Quantum Chemical Analysis

The optimized geometries and corresponding frontier molecular orbital (FMO) distributions of T1, T2, T3, and T4 are illustrated in Figure 2. Noticeable differences in electron density localization are observed among the investigated molecules, particularly in the spatial distribution of the highest occupied molecular orbital (HOMO). Compound T1 exhibits a more delocalized electron density across its molecular framework compared to the other derivatives, indicating enhanced electron-donating capability.

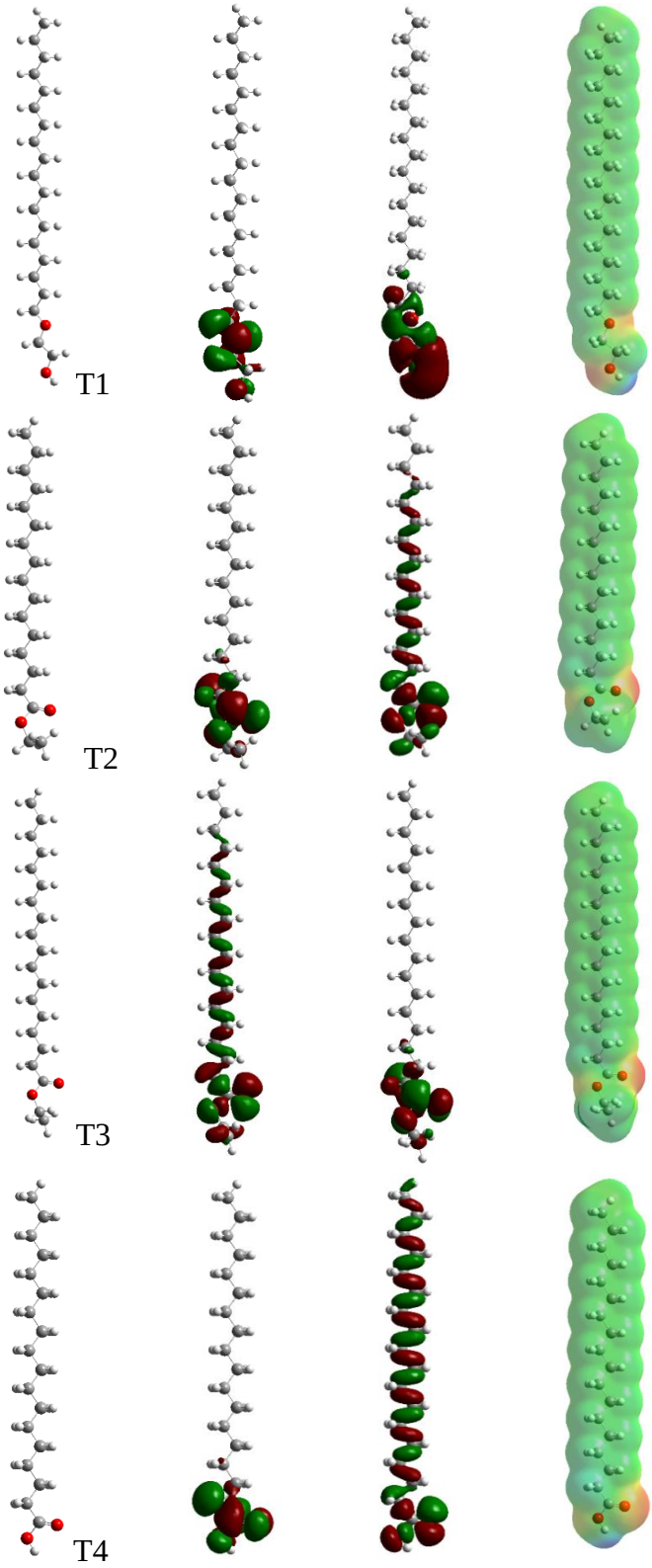

Figure 2. Visualization of the 2D structure, HOMO, LUMO, and ESP orbitals of T1, T2, T3, and T4.

Table 1. Quantum chemical parameters of T1, T2, T3, and T4 with B3LYP/6-311(d).

Parameter	Inhibitor			
	T1	T2	T3	T4
E_{HOMO} (eV)	-6.7114	-7.2241	-7.2216	-7.3509
E_{LUMO} (eV)	1.7921	0.3965	0.3981	0.2669
ΔE_{gab} (eV)	-8.5036	-7.6205	-7.6197	-7.6178
I (eV)	6.7114	7.2241	7.2216	7.3509
A (eV)	-1.7921	-0.3965	-0.3981	-0.2669
μ (Debye)	0.5015	1.4571	1.4536	1.4844
χ (eV)	2.4596	3.4138	3.4117	3.5419
η (eV)	4.2518	3.8103	3.8099	3.8089
σ (eV^{-1})	0.2352	0.2624	0.2625	0.2625

The HOMO distribution is primarily associated with regions containing oxygen atoms and long hydrocarbon chains, suggesting that these sites serve as potential adsorption centers for interaction with the aluminum surface. A higher EHOMO value generally reflects a stronger tendency of the molecule to donate electrons to the vacant orbitals of the metal, facilitating coordinate bond formation and surface adsorption. In this regard, the relatively elevated EHOMO of T1 supports its superior inhibition potential.

Furthermore, differences in electron density distribution influence molecular reactivity and adsorption orientation. Molecules with extended π-electron delocalization and accessible lone pair electrons typically exhibit stronger interaction with metallic substrates. The broader electron cloud in T1 enhances its ability to participate in donor–acceptor interactions, thereby reinforcing the predicted inhibition efficiency sequence derived from quantum descriptors.

Overall, the FMO analysis reveals that electronic structure characteristics strongly govern inhibitor performance, with T1 demonstrating the most favorable electron distribution pattern for adsorption and corrosion mitigation.

Global Reactivity Descriptors

The calculated quantum chemical parameters of T1, T2, T3, and T4 obtained at the B3LYP/6-311(d) level are summarized in Table 1. These descriptors provide quantitative insight into molecular reactivity, adsorption tendency, and predicted corrosion inhibition efficiency.

The EHOMO values indicate the electron-donating capability of the inhibitor molecules. Among the studied compounds, T1 exhibits the highest EHOMO value (–6.7114 eV), suggesting a stronger tendency to donate electrons to the vacant orbitals of the aluminum surface. Since adsorption onto metallic substrates is often facilitated by donor–acceptor interactions, a higher EHOMO generally correlates with enhanced inhibition performance. In contrast, T4 shows the lowest EHOMO (–7.3509 eV), implying comparatively weaker electron donation ability.

The energy gap ($|\Delta E|$ = ELUMO − EHOMO) serves as an indicator of molecular reactivity and chemical softness. T1 presents the largest absolute energy separation; however, its relatively favorable combination of frontier orbital energies enhances its donor interaction strength. Smaller energy gaps in T2–T4 suggest higher intrinsic reactivity, yet inhibition efficiency is not governed solely by ΔE but rather by the combined influence of electronic and adsorption parameters.

Ionization potential (I) and electron affinity (A) values further confirm that T1 requires less energy to donate electrons compared to the other derivatives. The electronegativity (χ) values reveal that T4 possesses the highest χ (3.5419 eV), indicating stronger electron-attracting character, whereas T1 shows the lowest χ (2.4596 eV), favoring electron donation toward the metal surface. Lower electronegativity difference between inhibitor and metal typically enhances charge transfer interactions.

Global hardness (η) and softness (σ = 1/η) provide additional insight into molecular polarizability. T1 exhibits the highest hardness (4.2518 eV) and correspondingly lower softness compared to the other derivatives, whereas T2–T4 demonstrate slightly higher softness values (~0.262 eV^{-1}), indicating marginally greater polarizability. Nevertheless, inhibition efficiency depends on balanced electronic

donation, molecular size, and adsorption capability rather than softness alone.

The dipole moment (μ) values suggest differences in molecular polarity. T4 presents the highest dipole moment (1.4844 Debye), while T1 has the lowest (0.5015 Debye). Although higher dipole moments may enhance interaction with polar environments, corrosion inhibition on metallic surfaces is more strongly influenced by frontier orbital characteristics and adsorption energetics than by polarity alone.
Overall, the combined analysis of EHOMO, electronegativity, ionization potential, and global reactivity parameters predicts the inhibition efficiency trend as: T1>T3≈T2>T4T1 > T3 approx T2 > T4T1>T3≈T2>T4

This theoretical ranking aligns with the adsorption energy trend obtained from Monte Carlo simulations, confirming the reliability of the integrated quantum–statistical modeling approach in predicting corrosion inhibition performance.

Monte Carlo Simulation Analysis

Monte Carlo (MC) simulations were conducted to evaluate the competitive adsorption behavior of inhibitor molecules and 100 water molecules on the Al(111) surface. The Al(111) crystallographic plane was selected due to its thermodynamic stability and dominant surface exposure in face-centered cubic aluminum, making it highly relevant for corrosion modeling. The simulation system consisted of one inhibitor molecule and an explicit aqueous environment to approximate realistic interfacial conditions.

Figure 3 illustrates the most stable adsorption configurations obtained after energy minimization and stochastic sampling. All investigated molecules (T1–T4) exhibit spontaneous adsorption onto the Al(111) surface, indicating thermodynamically favorable interaction. The adsorption distance between the active functional groups of the inhibitors and the metal surface was found to be below 3.5 Å in the most stable configurations, suggesting chemisorption-dominated interactions. Such short interaction distances indicate strong donor–acceptor coordination between electron-rich sites of the inhibitor molecules and vacant orbitals of surface aluminum atoms.

The calculated adsorption energies (Table 2) further confirm the strong affinity of the inhibitors toward the metal substrate. The magnitude of adsorption energy for each inhibitor–surface system is significantly higher (more negative) than that of water molecules alone, indicating preferential adsorption of organic inhibitors over solvent species. This competitive displacement of water molecules from the metal surface is a key requirement for effective corrosion inhibition.

Among the investigated derivatives, T1 exhibits the most negative adsorption energy (−3738.108 kcal•mol^{-1}), indicating the strongest binding interaction with the Al(111) surface in aqueous conditions. The adsorption strength follows the order: T1>T3>T2>T4

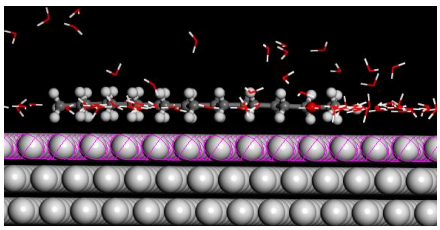

Al(111)/T1/100 H_2O

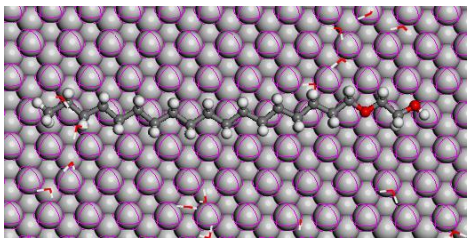

Al(111)/T1/100 H_2O

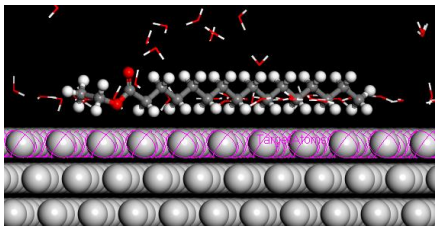

Al(111)/T2/100 H_2O

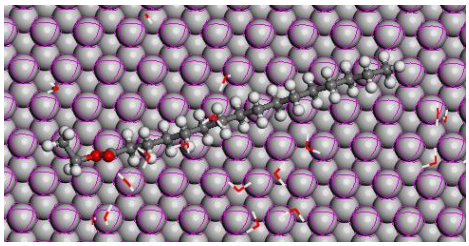

Al(111)/T2/100 H_2O

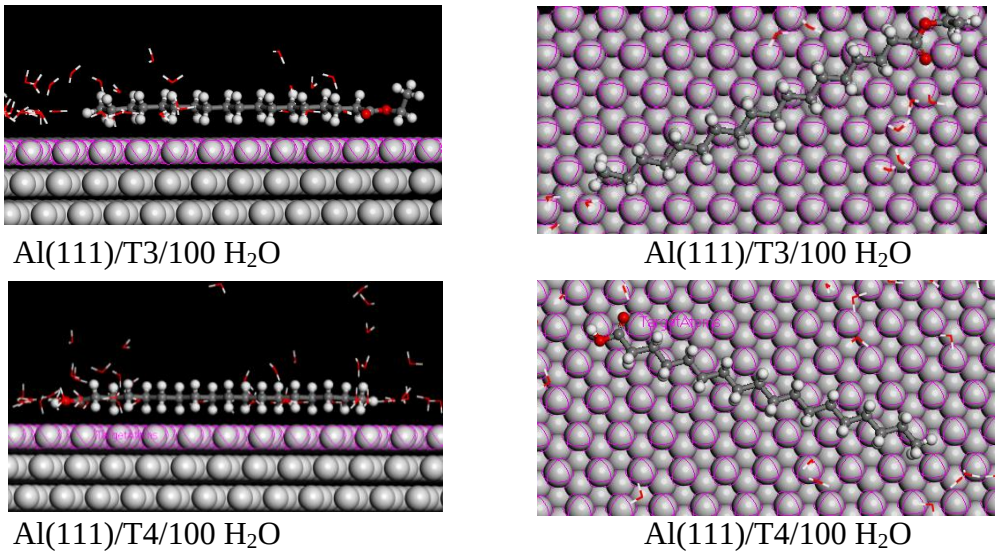

Figure 3. Adsorption of T1, T2, T3, and T4 on the surface of Al in the Monte Carlo Al(111)/inhibitor/100 H_2O system

Table 3. The energy of T1, T2, T3, and T4 adsorption and Al(111)/inhibitor/100 H_2O system derivatives based on Monte Carlo simulation.

Inhibitor	Adsorption Energy (kcal.mol^{-1})	Inhibitor (kcal.mol^{-1})	H_2O: dE_{ad}/dN_i (kcal.mol^{-1})
T1	-3738.108	-121.182	-28.416
T2	-3702.752	-102.512	-28.501
T3	-3717.256	-114.550	-28.765
T4	-3702.308	-111.655	-28.498

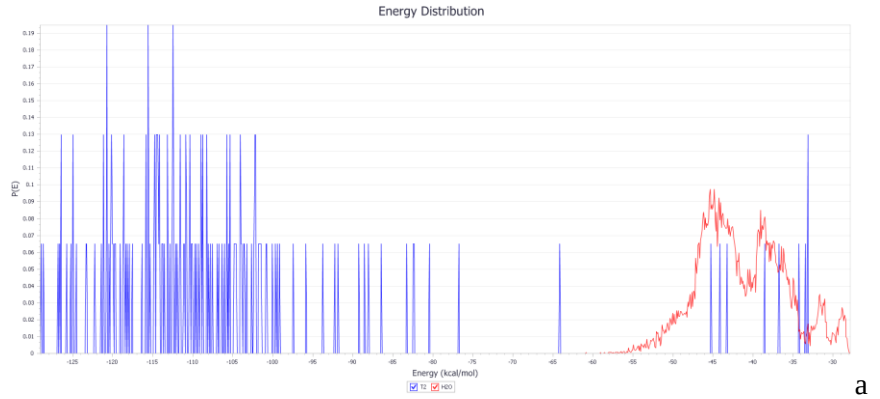

a

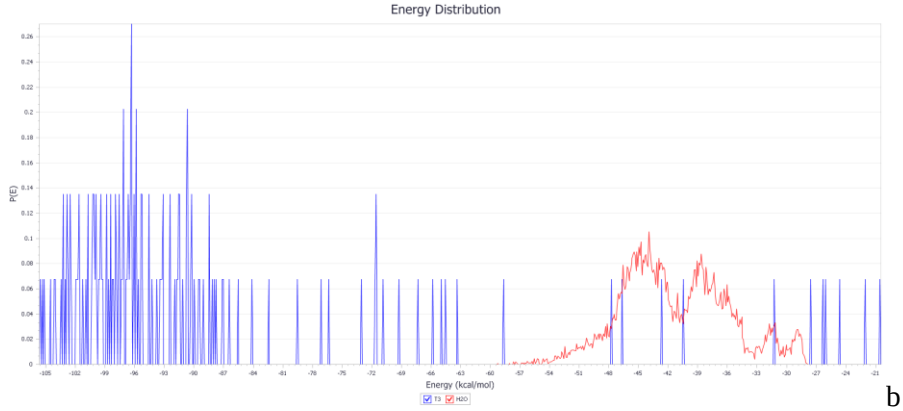

b

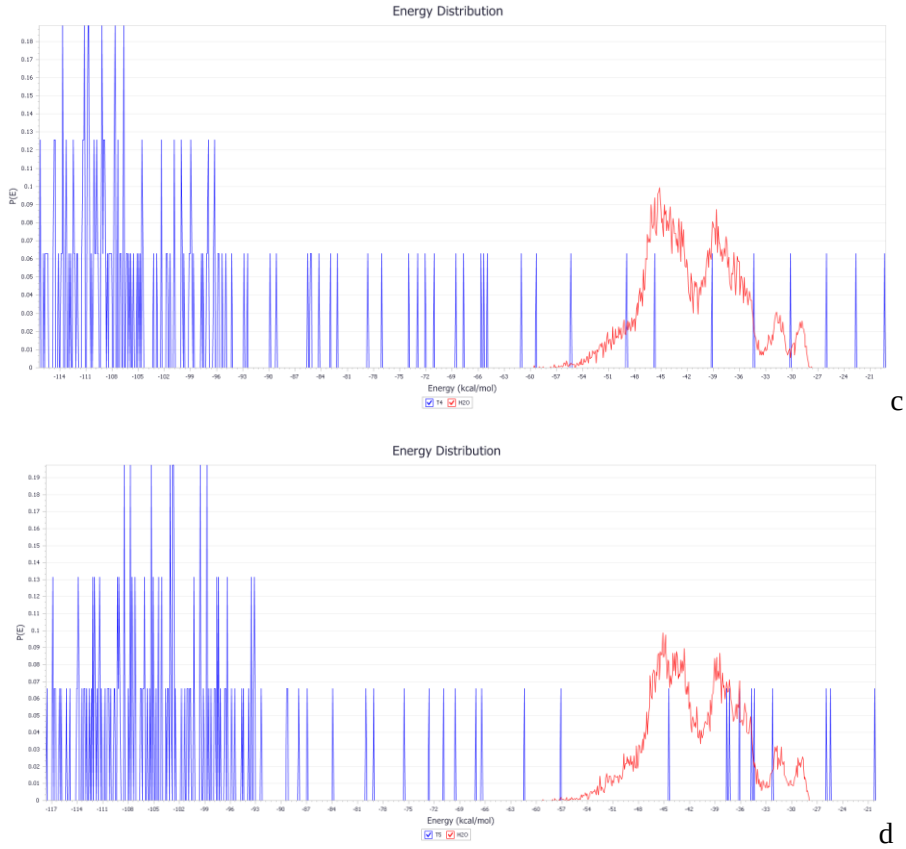

Figure 4. (a). Adsorption energy distribution for T1/100 H_2O, (b) T2/100 H_2O, (c) T3/100 H_2O, (d) T4 /100 H_2O

The larger negative adsorption energy of T1 suggests enhanced surface coverage, stronger interfacial stabilization, and the formation of a protective molecular layer capable of blocking active corrosion sites. In contrast, T4 shows comparatively weaker adsorption, consistent with its less favorable electronic descriptors obtained from DFT analysis.

Figure 4 presents the adsorption energy distribution profiles, demonstrating clear energetic separation between organic inhibitors and water molecules. The distinct distribution confirms that inhibitor adsorption dominates over solvent interaction, resulting in stable inhibitor–surface complexes. The strong adsorption of T1 is attributed to its favorable electronic properties, extended hydrocarbon chain, and effective surface orientation, which collectively promote stronger van der Waals and possible coordination interactions.

Overall, the MC simulation results validate the quantum chemical predictions and demonstrate that adsorption strength plays a decisive role in determining inhibition efficiency. The combined DFT–MC approach consistently identifies T1 as the most promising corrosion inhibitor for aluminum in aqueous environments.

Conclusion

This study presents a comprehensive theoretical investigation of selected organic derivatives from the ethanolic leaf extract of Sclerocarya birrea as potential green corrosion inhibitors for aluminum in aqueous environments. The inhibition performance of four major compounds—ethanol,2-(octadecyloxy) (T1), octadecanoic acid ethyl ester (T3), hexadecanoic acid ethyl ester (T2), and octadecanoic acid (T4)—was systematically evaluated using Density Functional Theory (DFT) at the B3LYP/6-311(d) level, complemented by ab initio MP2 analysis and Monte Carlo surface simulations. Quantum chemical descriptors revealed that molecular electronic properties strongly influence inhibition behavior, particularly frontier orbital energies and charge transfer capability. Monte Carlo simulations demonstrated spontaneous and energetically favorable adsorption of all

derivatives onto the Al(111) surface in the presence of water molecules, confirming their thermodynamic stability under aqueous conditions. The predicted inhibition efficiency consistently follows the order: T1 > T3 > T2 > T4. Among the investigated molecules, T1 exhibits the most favorable electronic characteristics and the highest adsorption energy, indicating superior surface affinity and protective layer formation. The integrated DFT–MP2–Monte Carlo framework employed in this work demonstrates the reliability of computational modeling in predicting corrosion inhibition performance prior to experimental validation. These findings provide a scientific basis for the rational design of sustainable, plant-derived corrosion inhibitors and offer valuable guidance for future experimental electrochemical studies and potential industrial-scale applications involving aluminum in aggressive aqueous media.

Acknowledgments

The authors gratefully acknowledge the productive academic collaboration between the Department of Chemical, Materials and Metallurgical Engineering, Botswana International University of Science and Technology (BIUST), Botswana. Their institutional support and cooperation have been invaluable to the completion of this research.

Conflicts of Interest

The authors declare that there are no conflicts of interest regarding the publication of this work.*Book*

References

1. Davis, J. R. (1999). Corrosion of aluminum and aluminum alloys. ASM International.
2. Hamid, M. K. A., Ishak, M. R., & Asyraf, M. R. M. (2021). Recent applications of aluminum alloys in aerospace and automotive industries. Materials Today: Proceedings, 46, 1991–1996.https://doi.org/10.1016/j.matpr.2020.09.601
3. Frankel, G. S. (1998). Pitting corrosion of aluminum alloys—A review of the critical factors. Journal of The Electrochemical Society, 145(6), 2186–2198.https://doi.org/10.1149/1.1838615
4. Abiola, A., & Otaigbe, J. (2008). The effects of temperature on corrosion of aluminium in acidic media. Corrosion Science, 50(9), 2429–2437. https://doi.org/10.1016/j.corsci.2008.06.009
5. Fontana, M. G. (1986). Corrosion engineering (3rd ed.). McGraw-Hill.
6. NACE International. (2016). International measures of prevention, application, and economics of corrosion technologies (IMPACT study). Corrosion, 72(8), 1000–1015. https://doi.org/10.5006/2173
7. Obot, I. B., & Obi-Egbedi, N. O. (2010). Adsorption properties and inhibition of mild steel corrosion in sulphuric acid solution by ketoconazole. Corrosion Science, 52(1), 198–204. https://doi.org/10.1016/j.corsci.2009.09.002
8. Umoren, S. A., & Obot, I. B. (2013). Eco-friendly corrosion inhibitors: Adsorption and inhibitive action of ethanol extracts of Andrographis paniculata leaves. Arabian Journal of Chemistry, 6(3), 343–352. https://doi.org/10.1016/j.arabjc.2010.11.004
9. Raja, P. B., & Sethuraman, M. G. (2008). Natural products as corrosion inhibitor for metals in corrosive media—A review. Materials Letters, 62, 113–116. https://doi.org/10.1016/j.matlet.2007.04.079
10. Quraishi, M. A., Singh, A., Singh, V. K., Yadav, D. K., & Singh, A. K. (2016). Green approach to corrosion inhibition of aluminum in acidic media using plant extracts. Journal of Molecular Liquids, 219, 1110–1116. https://doi.org/10.1016/j.molliq.2016.04.063
11. Khaled, K. F. (2010). Electrochemical investigation of corrosion and corrosion inhibition of aluminum in hydrochloric acid solution. Electrochimica Acta, 55, 6523–6532. https://doi.org/10.1016/j.electacta.2010.05.038
12. Ojewole, J. A. O., Mawoza, T., Chiwororo, W. D. H., & Owira, P. M. O. (2010). Sclerocarya birrea (A. Rich.) Hochst. [Anacardiaceae]: A review of its phytochemistry, pharmacology and toxicology and its ethnomedicinal uses. Phytotherapy Research, 24(5), 633–639. https://doi.org/10.1002/ptr.3080
13. Mariod, A. A., Matthäus, B., & Hussein, I. H. (2004). Chemical characterization of the seed and seed oil of Sclerocarya birrea (Marula) from Sudan. Journal of the American Oil Chemists' Society, 81(9), 827–

831. https://doi.org/10.1007/s11746-004-0986-9
14. Obot, I. B., Macdonald, D. D., & Gasem, Z. M. (2015). Density functional theory (DFT) as a powerful tool for designing new organic corrosion inhibitors. Corrosion Science, 99, 1–30. https://doi.org/10.1016/j.corsci.2015.01.037
15. Gece, G. (2008). The use of quantum chemical methods in corrosion inhibitor studies. Corrosion Science, 50(11), 2981–2992. https://doi.org/10.1016/j.corsci.2008.08.043
16. Verma, C., Ebenso, E. E., Quraishi, M. A., & Obot, I. B. (2018). Adsorption and corrosion inhibition performance of organic molecules: Multiscale modeling and experimental studies. Journal of Molecular Liquids, 260, 99–120. https://doi.org/10.1016/j.molliq.2018.03.045
17. Ebenso, E. E., Arslan, T., Kandemirli, F., Love, I., & Alemu, H. (2010). Quantum chemical studies of some rhodanine derivatives as corrosion inhibitors for mild steel in acidic medium. International Journal of Quantum Chemistry, 110(5), 1003–1018. https://doi.org/10.1002/qua.22181
18. Khaled, K. F., & Abdel-Rehim, S. S. (2011). Monte Carlo simulations of corrosion inhibition of mild steel in acidic solution by some organic compounds. Electrochimica Acta, 56(20), 6736–6745. https://doi.org/10.1016/j.electacta.2011.05.080
19. Zhang, D., Gao, L., & Zhou, G. (2008). Inhibition of copper corrosion in aerated hydrochloric acid solution by heterocyclic compounds: A quantum chemical and Monte Carlo simulation study. Corrosion Science, 50(12), 3615–3621. https://doi.org/10.1016/j.corsci.2008.09.024
20. Becke, A. D. (1993). Density-functional thermochemistry. III. The role of exact exchange. The Journal of Chemical Physics, 98(7), 5648–5652. https://doi.org/10.1063/1.464913
21. Lee, C., Yang, W., & Parr, R. G. (1988). Development of the Colle–Salvetti correlation-energy formula into a functional of the electron density. Physical Review B, 37(2), 785–789. https://doi.org/10.1103/PhysRevB.37.785
22. Hehre, W. J., Ditchfield, R., & Pople, J. A. (1972). Self-consistent molecular orbital methods. XII. Further extensions of Gaussian-type basis sets for use in molecular orbital studies of organic molecules. The Journal of Chemical Physics, 56(5), 2257–2261. https://doi.org/10.1063/1.1677527
23. Frisch, M. J., Trucks, G. W., Schlegel, H. B., et al. (2009). Gaussian 09, Revision D.01. Gaussian, Inc.
24. Koopmans, T. (1934). Über die Zuordnung von Wellenfunktionen und Eigenwerten zu den einzelnen Elektronen eines Atoms. Physica, 1(1–6), 104–113. https://doi.org/10.1016/S0031-8914(34)90011-2
25. Parr, R. G., & Yang, W. (1985). Density functional approach to the frontier-electron theory of chemical reactivity. Journal of the American Chemical Society, 107(25), 7312–7316. https://doi.org/10.1021/ja00310a022
26. Pearson, R. G. (1988). Absolute electronegativity and hardness: Applications to organic chemistry. Journal of Organic Chemistry, 53(5), 1072–1077. https://doi.org/10.1021/jo00239a034
27. Pearson, R. G. (1990). Hard and soft acids and bases—The evolution of a chemical concept. Coordination Chemistry Reviews, 100, 403–425. https://doi.org/10.1016/0010-8545(90)85016-L
28. Gece, G. (2008). The use of quantum chemical methods in corrosion inhibitor studies. Corrosion Science, 50(11), 2981–2992. https://doi.org/10.1016/j.corsci.2008.08.043
29. Obot, I. B., Macdonald, D. D., & Gasem, Z. M. (2015). Density functional theory (DFT) as a powerful tool for designing new organic corrosion inhibitors. Corrosion Science, 99, 1–30. https://doi.org/10.1016/j.corsci.2015.01.037